PROCEEDINGS OF SCIENCE

SST-1M Observations of Markarian 421

S. R. Muthyala,[a,*] A. Araudo,[a] J. Juryšek[a] and A. L. Müller[a] for the SST-1M Collaboration

[a] *FZU - Institute of Physics of the Czech Academy of Sciences, Na Slovance 1999/2, Prague 8, Czech Republic*

E-mail: muthyala@fzu.cz

Markarian 421 (Mrk 421) is the closest and one of the brightest high-frequency peaked blazars, located at a redshift of z = 0.031. It is a strong source of gamma rays, and its broadband emission has been extensively studied over the years through multi-wavelength observations. Mrk 421 has been the target of an observational campaign from January to May 2024, with 23 nights of observation conducted by the SST-1M telescopes – two single-mirror, small-size Cherenkov telescopes at the Ondřejov Observatory, Czech Republic. These telescopes operate in mono and stereoscopic modes, utilizing the imaging atmospheric Cherenkov technique to detect very high-energy gamma rays in the 1–300 TeV energy range. Using about 32.92 hours of data collected by the telescopes in stereo mode, we find that the gamma-ray spectrum above 1 TeV is well described by a power-law function with an index of 3.24 ± 0.26. In this work, we present our recent SST-1M stereo observations, data analysis, and the results of preliminary physical modeling of Mrk 421's emission mechanisms.

39th International Cosmic Ray Conference (ICRC2025)
15–24 July 2025
Geneva, Switzerland

ICRC 2025
The Astroparticle Physics Conference
Geneva July 15-24, 2025

*Speaker

PoS(ICRC2025)776

1. Introduction

Observations of very high-energy (VHE) gamma rays can shed light on extreme particle acceleration processes in the Universe. At these energies ($E \gtrsim 0.1$ TeV), gamma rays cannot be directly detected by ground-based telescopes due to atmospheric absorption. While space-based instruments such as Fermi-LAT can efficiently detect photons up to 300 GeV, gamma-ray sources above this energy have fluxes too low for direct detection from space, which would require instruments of impractically large size. Instead, VHE gamma rays are observed indirectly by ground-based telescopes through Cherenkov radiation produced by charged particles in extensive air showers, resulting from the interactions of gamma-ray photons with atmospheric nuclei.

Blazars are the most commonly detected class of VHE gamma-ray sources in the extragalactic sky. They are a classification of radio-loud active galactic nuclei (AGN) characterized by ultra-relativistic jets emanating from the supermassive black hole that are oriented along or very close to the line of sight. Due to relativistic beaming, the jet pointing toward the observer appears highly boosted and often dominates the observed emission across the entire electromagnetic spectrum, while the counter-jet is typically undetectable. Their spectral energy distribution (SED) is characterized by two energy peaks. The first peak at the low to medium energy range of Radio to X-rays is produced by the synchrotron emission from relativistic electrons embedded in the magnetic field of the jet, while the second peak at the high energies of gamma-rays is thought to be produced by synchrotron self-Compton (SSC) emission [1]. Based on the position of the synchrotron peak, these sources are subclassified as low synchrotron peaked (LSP) blazars if the peak frequency is less than 10^{14} Hz, or high synchrotron peaked (HSP) blazars if the frequency is larger than 10^{14} Hz.

Markarian 421 (Mrk 421) is an HSP blazar and a strong gamma-ray emitter. It is the closest and one of the brightest blazars, at a redshift $z = 0.031$. Mrk 421 is a highly variable source, and the source is extensively studied to understand its broadband emission, yet the mechanisms underlying blazar emission are still not firmly established. The main limitations arise from insufficient multi-frequency coverage and the moderate sensitivity of previous gamma-ray measurements. Moreover, the majority of prior observations have been concentrated on episodes of high activity or flaring states, leaving quiescent phases underexplored. Enhanced sensitivity and detailed observations of non-flaring states are thus crucial for closing existing gaps in the multi-wavelength characterization of Mrk 421.

Figure 1: LEFT: SST-1M telescope 1 in the Ondřejov Observatory near Prague. RIGHT: An aerial view of the two SST-1M telescopes located 155.2 m apart (C. Alispach et al., 2025).

In this contribution, we present the first SST-1M observations of Mrk 421, conducted between January and May 2024, and derive a preliminary model of emission using the averaged SED. The SST-1M is a single-mirror small-size Cherenkov telescope designed by a consortium of institutes from Poland, Switzerland, and the Czech Republic to detect VHE gamma-ray-induced atmospheric showers in the 3-300 TeV range (see Fig. 1). Each telescope has a 4-m diameter, multi-segmented mirror dish composed of 18 hexagonal facets, along with a high-performance SiPM-based camera with a wide optical field of view of 9 degrees [2].

Currently, two SST-1M telescopes are installed at the Ondřejov Observatory in the Czech Republic, where they can operate in mono mode or, taking advantage of their relative distance of 155.2 m, detect air showers stereoscopically (see right panel of Fig. 1) [3]. Their timestamps are synchronized to nanosecond precision using the White Rabbit timing network [4]. The geometrical and timing properties of the detected signals are used to find the physical properties of the primary particle. The raw signals are calibrated and processed up to the photon list with reconstructed energies and arrival directions (see [3], for the details of the analysis and reconstruction) using the standard data processing and analysis tool developed for SST-1M, `sst1mpipe`[1] [5]. The telescopes are also designed for remote operation. This work focuses on observations of Mrk 421 in the VHE gamma-ray domain with the newly developed SST-1M stereoscopic system, with the objective of providing enhanced results to complement existing studies.

2. Data Acquisition and Analysis

For observation and data taking, we follow the wobble technique, which allows us to determine the background from the same data set as the signal events [6]. During this period, the telescopes collected raw data over 23 nights, corresponding to an effective exposure of 51.10h in stereoscopic mode. When the gamma-ray shower triggers the SST-1M telescope, the entire waveform of 50 samples with 4 ns binning is stored. During data analysis in `sst1mpipe`, the waveform in each camera pixel is calibrated, integrated, and cleaned from background noise to obtain the image parameters. For these cleaned images, Random Forests trained on the Monte Carlo simulations are applied to each event to get the final parameters of the primary particles, including the so-called gammaness, describing how gamma-like a given shower image is. An energy-dependent cut on gammaness is applied to obtain the final photon list. In the current work, we use the energy-dependent gammaness cut on 50% gamma efficiency in all energy bins to get the final sample. From the final photon list, we can derive the fluxes and energies to construct SEDs and skymaps. Since the atmospheric conditions at Ondřejov are highly variable, we apply data quality cuts to obtain a high-quality data set. Data affected by bad atmospheric conditions, such as highly variable night sky background (NSB), clouds, auroras, and technical issues, is removed. After the data selection, the final data set used for our analysis consists of about 32.92 hours of stereo data.

The significance map in the left panel of Figure 2 quantifies the statistical probability of observing the signal at a particular location in the sky. The excess map in the middle panel of Figure 2 shows the difference between the observed gamma-ray counts and the expected background counts. The maps are produced using the 'ring background method' in the Python package `gammapy`

[1] https://github.com/SST-1M-collaboration/sst1mpipe

[7]. Here, a ring with radius 0.7° and width 0.3° was used to estimate background events, and a region of 0.3° around Mrk 421 was excluded from the background estimation. The source was detected during the observations of 32.9 hours with a total significance of 16.62 and excess counts of 142. The distribution of local significance in the right panel of Figure 2 shows that the background/off-region can be described by a Gaussian function, and the excess counts show the presence of the source. The background distribution is fitted by a Gaussian with a mean of −0.14 and a standard deviation of 1.03, which is consistent with theoretical expectations for an unbiased background.

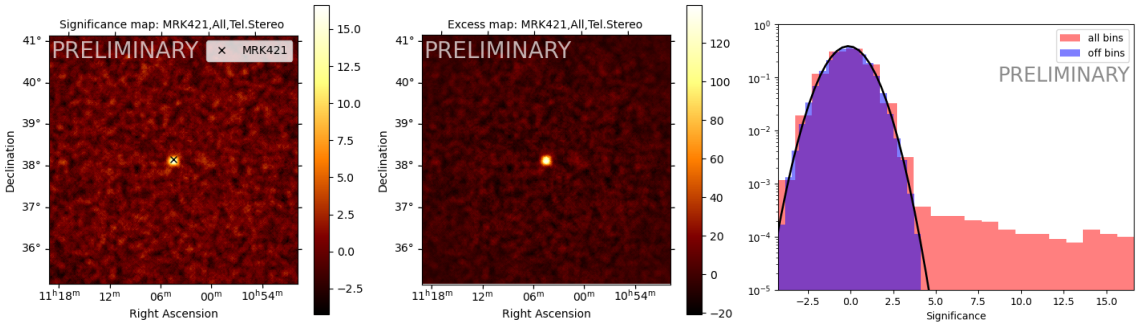

Figure 2: LEFT: Significance map. MIDDLE: Excess map of Mrk 421 in stereo mode. RIGHT: 1D distribution of significance in stereo mode.

We also used `gammapy` to perform 1D spectral analysis using the reflected background method. The forward folding method is used to reconstruct the gamma-ray spectrum observed by the telescope. For every night, we reconstruct the spectrum using a Power Law (PL) spectral model $\mathrm{d}N/\mathrm{d}E = A(E/3\,\mathrm{TeV})^{-\alpha}$, where α stands for spectral index and A for the flux normalization at 3 TeV. In Figure 3 we show the light curve of Mrk 421 using the function LightCurveEstimator from `gammapy`. We obtain an average flux for energies above 1 TeV of $F = (8.01 \pm 2.54) \times 10^{-14}$ $\mathrm{TeV}^{-1}\mathrm{cm}^{-2}\mathrm{s}^{-1}$. In the figure, flux data points are represented by orange markers, and the black line represents the average flux. Note that no flares are detected in this observation period [2] (see however, [8]).

The preliminary spectrum of Mrk 421, reconstructed from the final stereo-mode dataset, is shown in Figure 4. The figure displays the observed and intrinsic spectra, both fitted with a PL model, in blue and green, respectively. The shaded bands represent the statistical uncertainties of the fits, while the flux points and upper limits are overlaid in matching colors. As the VHE gamma rays from distant sources do not reach Earth unaltered, the observed spectrum must be corrected for absorption processes occurring during their propagation. In particular, gamma rays interact with the low-energy photons of the Extragalactic Background Light (EBL), producing electron–positron pairs and effectively dimming the signal, thereby reducing the number of gamma rays that actually reach our telescopes and making the observed spectrum appear softer than the true emission of the source. The intrinsic spectrum of Mrk 421 was therefore reconstructed using the EBL model

[2] Typically, for a flare, the peak flux should be more than three times the standard deviation of the average flux in a band.

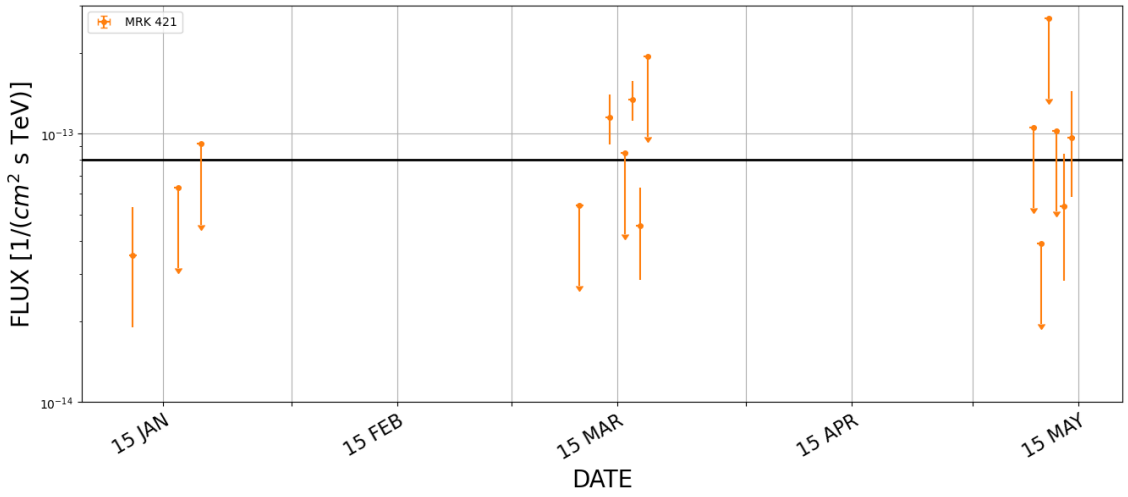

Figure 3: SST-1M Light Curve of Mrk 421 in stereo mode. In the figure, the black line represents the average flux above 1 TeV, and the orange flux data points and upper limits.

proposed by Franceschini (2007) [9], which estimates this absorption effect. The best-fit parameters of intrinsic spectra are shown in Table 1.

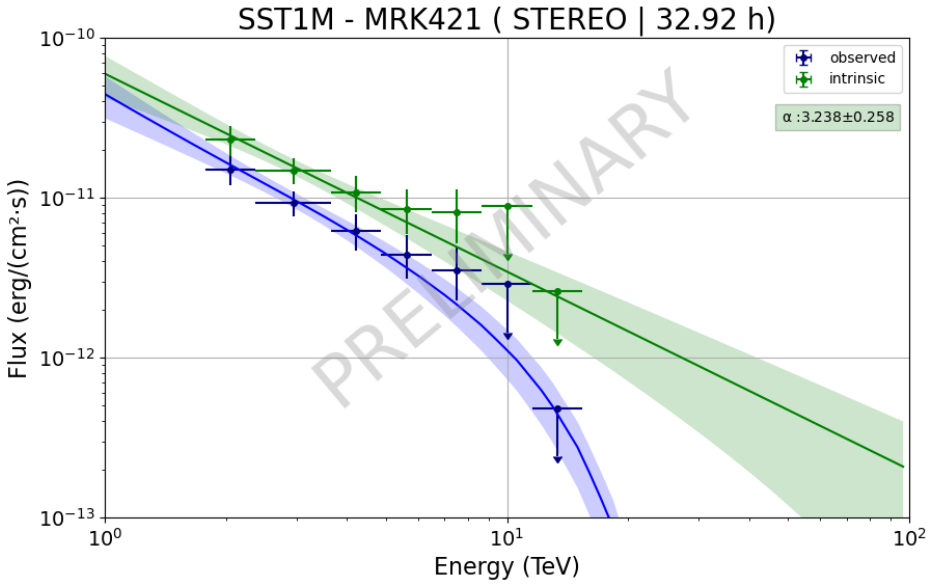

Figure 4: Energy spectrum of Mrk 421 in stereo mode, showing both observed (blue) and intrinsic (green) spectra fitted with a PL model.

Best fit parameters	Power law index	Amplitude ($TeV^{-1}cm^{-2}s^{-1}$)
Intrinsic Spectrum	3.24 ± 0.26	$(1.06 \pm 0.12) \times 10^{-12}$

Table 1: Best fit parameters for the intrinsic spectra of Mrk 421 obtained using a PL model.

3. Data Modeling

HSP blazars are low-luminosity sources characterized by their first SED peak in the UV–X-ray band, where most of their power is emitted. As a result, the synchrotron hump is shifted to higher frequencies compared to other blazar types. In these systems, the seed photons available for inverse-Compton scattering at VHE are synchrotron photons, making the SSC framework the standard model for describing the high-energy part of the SED. Previous studies show a good fit for the low-energy component from radio to X-rays and high-energy component in the GeV range of gamma-rays, but a poor fit for the high-energy tail in the TeV regime, usually due to a lack of sufficient data (see e.g.,[1] and [10]). In this study, we aim to improve the fitting of the high-energy tail of Mrk 421 with the addition of new data observed by SST-1M at photon energies greater than 2 TeV to the existing dataset from the literature.

Following [1], we use the Python package `agnpy` with `gammapy` as the wrapper to model the broad-band SED of the blazar Mrk 421, assuming the emission is produced by synchrotron and SSC emission [11]. We consider a broken power law for the distribution of relativistic electrons with a minimum energy of $500 m_e c^2$. The data consists of observed data from SST-1M combined with the time-averaged SED of Mrk 421 from Abdo et al (2011a) [12], which contains multi-frequency data from several instruments covering the energy range from radio to gamma rays, observed during the time period of January 19 to June 1, 2009. In their study, the data were corrected for host galaxy emission subtraction, galactic extinction correction for optical/x-ray data, and TeV data were corrected for absorption in EBL using the model in [9]. The best fit corresponds to a Doppler factor of $\delta_D = 24.29 \pm 0.01$, giving the value of radius emission zone as $R = 6.1 \times 10^{16}$ cm using values of redshift as $z = 0.031$ and the variability time scale of 1 day. In our model, we use an electron distribution that follows a broken power law with energy break of $E_{\rm b} = 59.08 \pm 0.51$ GeV and spectral indexes before and after the break of $p_1 = 2.11 \pm 0.01$ and $p_2 = 3.38 \pm 0.10$, respectively. The maximum electron energy of the best fit is given by $E_{\rm max} = 557.47 \pm 0.58$ GeV. The magnetic field results in a value of B = 24.58 ± 1.01 mG. In Figure 5, we show the multi-frequency SED of Mrk 421 (data points) and the best SSC model (black line). Table 2 shows a summary of the best-fit parameters, which are in good agreement with previous results [1].

Parameter	Symbol	Mrk 421
Doppler factor	δ_D	24.29 ± 0.01
Magnetic field	B [mG]	24.58 ± 1.01
Spectral index before break	α_1	2.11 ± 0.01
Spectral index after break	α_2	3.38 ± 0.10
Energy break	$E_{\rm b}$ [GeV]	59.08 ± 0.51
Maximum electron energy	$E_{\rm max}$ [GeV]	557.47 ± 0.58

Table 2: Best fit parameters for the SSC model of Mrk 421 using `agnpy`.

4. Conclusions

We present the preliminary results of the first set of observations of Mrk 421 taken by SST-1M telescopes in stereo mode from January to May 2024, with about 33 high-quality hours of

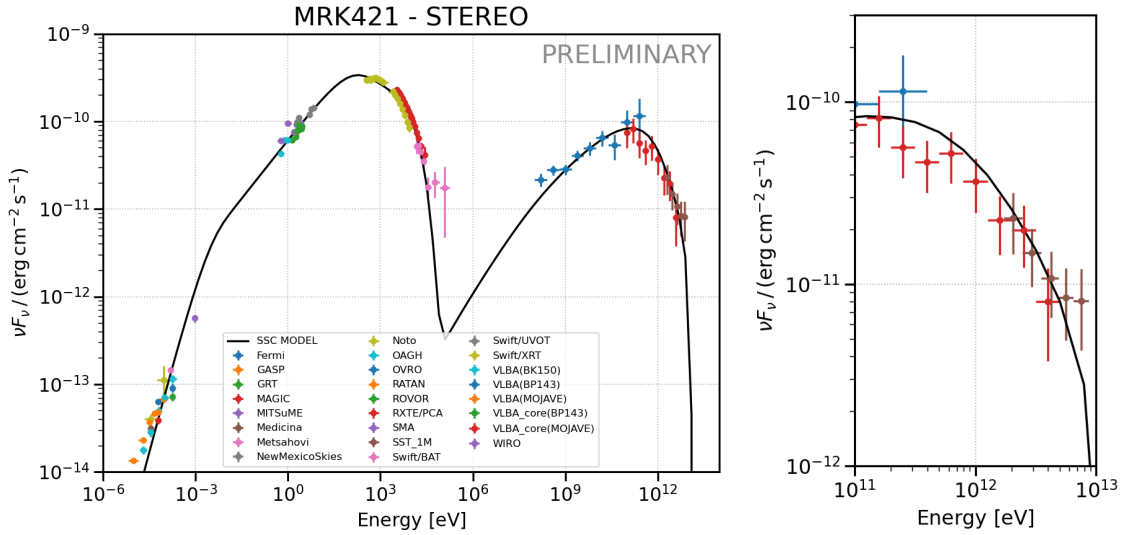

Figure 5: LEFT: SED of Mrk 421 with best fit SSC model using `agnpy` package. RIGHT: Zoomed figure showing the VHE part of the SED in the TeV energy range with data from points from Fermi (in blue), MAGIC (in red), and SST-1M (in brown).

observation. We obtain an intrinsic energy spectrum of Mrk 421 by fitting a PL model with an index of 3.24 ± 0.26 and an amplitude of $(1.06 \pm 0.12) \times 10^{-12}$ TeV^{-1} cm^{-2} s^{-1}, at a reference energy of 3 TeV. The significance and excess maps produced using the 'ring background method' show that the source was clearly detected during the observations with a total significance of 16.62 σ and excess counts of 142. The best-fit parameters of the SED modeling of Mrk 421, including our stereo data, are in good agreement with previous results when the standard blazar scenario of synchrotron self-Compton emission is considered. In a further study, we will focus on improving the SED by adding the data from HAWC [1], and more simultaneous data from other instruments at different energies to build a time-averaged SED model of Mrk 421.

5. Acknowledgments

This publication was created as part of the projects funded in Poland by the Minister of Science based on agreements number 2024/WK/03 and DIR/WK/2017/12. The construction, calibration, software control, and support for operation of the SST-1M cameras are supported by SNF (grants CRSII2_141877, 20FL21_154221, CRSII2_160830, _166913, 200021-231799), by the Boninchi Foundation, and by the Université de Genève, Faculté de Sciences, Département de Physique Nucléaire et Corpusculaire. The Czech partner institutions acknowledge support of the infrastructure and research projects by the Ministry of Education, Youth and Sports of the Czech Republic (MEYS) and the European Union funds (EU), MEYS LM2023047, EU/MEYS CZ.02.01.01/00/22_008/0004632, CZ.02.01.01/00/22_010/0008598, Co-funded by the European Union (Physics for Future – Grant Agreement No. 101081515), and Czech Science Foundation, GACR 23-05827S.

References

[1] A. Albert, R. Alfaro, C. Alvarez, J.R. Angeles Camacho, J.C. Arteaga-Velázquez, K.P. Arunbabu et al., Long-term Spectra of the Blazars Mrk 421 and Mrk 501 at TeV Energies Seen by HAWC, Astrophyical Journal **929** (2022) 125 [2106.03946].

[2] C. Alispach, A. Araudo, M. Balbo, V. Beshley, A. Biland, J. Blažek et al., The SST-1M imaging atmospheric Cherenkov telescope for gamma-ray astrophysics, JCAP **2025** (2025) 047 [2409.11310].

[3] C. Alispach, A. Araudo, M. Balbo, V. Beshley, J. Blažek, J. Borkowski et al., Observation of the crab nebula with the single-mirror small-size telescope stereoscopic system at low altitude, 2506.01733.

[4] J. Serrano et al., The White Rabbit Project, in ICALEPCS, Kobe, Japan, 12th International Conference on Accelerator and Large Experimental Physics Control Systems, 2009.

[5] J. Jurysek et al., Sst-1m-collaboration/sst1mpipe: v0.7.3, Feb., 2025. 10.5281/zenodo.14808846.

[6] V.P. Fomin, A.A. Stepanian, R.C. Lamb, D.A. Lewis, M. Punch and T.C. Weekes, New methods of atmospheric Cherenkov imaging for gamma-ray astronomy. I. The false source method, Astroparticle Physics **2** (1994) 137.

[7] A. Donath et al., gammapy/gammapy: v.0.19, Nov., 2021. 10.5281/zenodo.5721467.

[8] T. Tavernier and SST-1M Consortium, Detection of enhanced very-high-energy gamma-ray emission from Markarian 421, The Astronomer's Telegram **16533** (2024) 1.

[9] A. Franceschini and G. Rodighiero, The extragalactic background light revisited and the cosmic photon-photon opacity, Astronomy and Astropysics **603** (2017) A34 [1705.10256].

[10] Z.-R. Wang, R. Xue, D. Xiong, H.-Q. Wang, L.-M. Sun, F.-K. Peng et al., Broadband Multiwavelength Study of LHAASO-detected Active Galactic Nuclei, **271** (2024) 10 [2308.10200].

[11] C. Nigro, J. Sitarek, P. Gliwny, D. Sanchez, A. Tramacere and M. Craig, agnpy: An open-source python package modelling the radiative processes of jetted active galactic nuclei, Astronomy and Astropysics **660** (2022) A18 [2112.14573].

[12] A.A. Abdo, M. Ackermann, M. Ajello, L. Baldini, J. Ballet, G. Barbiellini et al., Fermi large area telescope observations of markarian 421: The missing piece of its spectral energy distribution, The Astrophysical Journal **736** (2011) 131.

Full Authors List: SST-1M Collaboration

C. Alispach[1], A. Araudo[2], M. Balbo[1], V. Beshley[3], J. Blažek[2], J. Borkowski[4], S. Boula[5], T. Bulik[6], F. Cadoux[‘], S. Casanova[5], A. Christov[2], J. Chudoba[2], L. Chytka[7], P. Čechvala[2], P. Dědic[2], D. della Volpe[1], Y. Favre[1], M. Garczarczyk[8], L. Gibaud[9], T. Gieras[5], E. Głowacki[9], P. Hamal[7], M. Heller[1], M. Hrabovský[7], P. Janeček[2], M. Jelínek[10], V. Jílek[7], J. Juryšek[2], V. Karas[11], B. Lacave[1], E. Lyard[12], E. Mach[5], D. Mandát[2], W. Marek[5], S. Michal[7], J. Michałowski[5], M. Miroń[9], R. Moderski[4], T. Montaruli[1], A. Muraczewski[4], S. R. Muthyala[2], A. L. Müller[2], A. Nagai[1], K. Nalewajski[5], D. Neise[13], J. Niemiec[5], M. Nikołajuk[9], V. Novotný[2,14], M. Ostrowski[15], M. Palatka[2], M. Pech[2], M. Prouza[2], P. Schovanek[2], V. Sliusar[12], Ł. Stawarz[15], R. Sternberger[8], M. Stodulska[1], J. Świerblewski[5], P. Świerk[5], J. Štrobl[10], T. Tavernier[2], P. Trávníček[2], I. Troyano Pujadas[1], J. Vícha[2], R. Walter[12], K. Ziętara[15]

[1]Département de Physique Nucléaire, Faculté de Sciences, Université de Genève, 24 Quai Ernest Ansermet, CH-1205 Genève, Switzerland. [2]FZU - Institute of Physics of the Czech Academy of Sciences, Na Slovance 1999/2, Prague 8, Czech Republic. [3]Pidstryhach Institute for Applied Problems of Mechanics and Mathematics, National Academy of Sciences of Ukraine, 3-b Naukova St., 79060, Lviv, Ukraine. [4]Nicolaus Copernicus Astronomical Center, Polish Academy of Sciences, ul. Bartycka 18, 00-716 Warsaw, Poland. [5]Institute of Nuclear Physics, Polish Academy of Sciences, PL-31342 Krakow, Poland. [6]Astronomical Observatory, University of Warsaw, Al. Ujazdowskie 4, 00-478 Warsaw, Poland. [7]Palacký University Olomouc, Faculty of Science, 17. listopadu 50, Olomouc, Czech Republic. [8]Deutsches Elektronen-Synchrotron (DESY) Platanenallee 6, D-15738 Zeuthen, Germany. [9]Faculty of Physics, University of Białystok, ul. K. Ciołkowskiego 1L, 15-245 Białystok, Poland. [10]Astronomical Institute of the Czech Academy of Sciences, Fričova 298, CZ-25165 Ondřejov, Czech Republic. [11]Astronomical Institute of the Czech Academy of Sciences, Boční II 1401, CZ-14100 Prague, Czech Republic. [12]Département d’Astronomie, Faculté de Science, Université de Genève, Chemin d’Ecogia 16, CH-1290 Versoix, Switzerland. [13]ETH Zurich, Institute for Particle Physics and Astrophysics, Otto-Stern-Weg 5, 8093 Zurich, Switzerland. [14]Institute of Particle and Nuclear Physics, Faculty of Mathematics and Physics, Charles University, V Holešovičkách 2, Prague 8, Czech Republic. [15]Astronomical Observatory, Jagiellonian University, ul. Orla 171, 30-244 Krakow, Poland.